

University of Bern, Laboratory for High Energy Physics  
preprint BUHE-9906

## CRYOGENIC CALORIMETERS IN ASTRO AND PARTICLE PHYSICS

K.PRETZL

*Laboratory for High Energy Physics of the University Bern, Sidlerstr. 5  
CH 3012 Bern, Switzerland E-mail:Pretzl@lhep.unibe.ch*

The development of cryogenic calorimeters was originally motivated by the fact that very low energy thresholds and excellent energy resolutions can be achieved by these devices. Cryogenic devices are widely used in double beta decay experiments, in cosmological dark matter searches, in x-ray detection of galactic and extragalactic objects as well as in cosmic background radiation experiments. An overview of the latest developments is given.

### 1 Introduction

Cryogenic calorimeters open up the possibility of measuring processes with energy transfers as low as eV with very high accuracy. Their development has recently been motivated by the quest for the dark matter in the universe and for the missing neutrinos from the sun. Other research areas have also benefitted from these developments, such as the double  $\beta$ -decay experiments, neutrino mass experiments, x-ray spectroscopy in astrophysics, single photon counting spectrometry, mass spectrometry of large molecules (DNA sequencing) as well as x-ray microanalysis for industrial applications.

### 2 First Ideas and Attempts

In 1935 F.Simon <sup>1</sup> suggested measuring the energy deposited by radioactivity with cryogenic calorimeters. Later in 1949 D.H.Andrews, R.D.Fowler and M.C.Williams <sup>2</sup> reported the detection of individual  $\alpha$ -particles using a superconducting strip. G.H.Wood and B.L.White <sup>3</sup> detected  $\alpha$ -particles with a superconducting tunnel junction (STJ) detector. H.Bernas et al. <sup>4</sup> used superheated superconducting granules (SSG) for beta radiation. A.K.Drukier

and C.Vallette detected charged particles with SSG <sup>5</sup>. T.Niinikoski and F.Udo <sup>6</sup> proposed cryogenic calorimeters for the detection of neutrinos in 1974. E.Fiorini and T.O.Niinikoski <sup>7</sup> explored in 1983 the possibility of low temperature calorimetry to improve the limits on processes such as neutrinoless double-beta decay. A.Drukier and L.Stodolsky <sup>8</sup> suggested 1984 the use of SSG detectors for neutrino-physics and astrophysics experiments. With all these interesting first ideas and experimental attempts in mind, a first workshop (LTD1) <sup>9</sup> on low temperature detectors was organized in 1987 at Ringberg-Kastell on Lake Tegernsee in southern Bavaria. Many of these ideas have been shown to work and the field has been successfully growing and reaching many areas of research. Subsequent workshops were held in Annecy (France) LTD2 <sup>10</sup>, the Gran Sasso Laboratory (Italy) LTD3 <sup>11</sup>, Oxford (Great Britain) LTD4 <sup>12</sup>, Berkeley (USA) LTD5 <sup>13</sup>, Beatenberg (Switzerland) LTD6 <sup>14</sup> and Munich (Germany) LTD7 <sup>15</sup>. The eighth in this series of workshops LTD8 will be held in Dalfsen (Netherlands)(15-20 August 1999). Much of the original work in this field can be found in the proceedings of these workshops as well as in <sup>16</sup>. There are also excellent review articles on the subject <sup>17,18,19,20</sup>.

### 3 Why Cryogenic Detectors?

Most calorimeters used in high energy physics measure the energy loss of a particle in form of ionization or scintillation light. In contrast, cryogenic calorimeters are able to measure the total deposited energy in form of ionization and heat. This feature makes them very effective in detecting very small energy deposits with high resolution. A small energy loss  $\Delta E$  of a particle can lead to an appreciable temperature increase  $\Delta T$  in the calorimeter

$$\Delta T = \frac{\Delta E}{C_{tot}} \quad (1)$$

provided the heat capacity  $C_{tot} = cV$  of a calorimeter with a given volume  $V$  is small. A condition which can be reached at low temperatures due to the rapid decrease of the specific heat  $c$  with temperature

for a dielectric crystal

$$c = \beta \left[ \frac{T}{\Theta_D} \right]^3 \quad (2)$$

for a normal conductor

$$c = \beta \left[ \frac{T}{\Theta_D} \right]^3 + \gamma T \quad (3)$$

for a superconductor

$$c = \beta \left[ \frac{T}{\Theta_D} \right]^3 + \alpha e^{\Delta/kT} \quad (4)$$

where  $\alpha, \beta, \gamma$  are material dependent parameters,  $\Theta_D$  is the Debye temperature and  $\Delta$  is the energy gap of the superconductor with a typical value of the order of 1meV.

In Fig.1 a typical cryogenic calorimeter is shown. It consists of an absorber with heat capacity  $C$ , a thermometer and a thermal link with heat conductance  $g$  to a heat reservoir with constant bath temperature  $T_B$ . Particles interacting in the absorber cause a change in the resistance of the thermometer. This is measured by observing a voltage drop across it when passing a current  $I$  through the thermometer.

Cryogenic calorimeters can be made from many different materials including superconductors, a feature which turns out to be very useful for many applications. They can be used as targets and detectors at the same time. Due to the very small energy quanta involved they reach much higher energy resolutions than conventional devices. For example, it takes only of the order of 1meV to break a Cooper pair in a superconductor whereas a few eV are needed to create an electron-hole pair in a solid-state device.

#### 4 Energy Resolution

The mean energy fluctuation in an absorber with a thermal link to the heat sink is:

$$\Delta E_{FWHM} = 2.35\xi\sqrt{kT^2C} \quad (5)$$

It is independent of the absorbed energy and the thermal conductance of the link.  $\xi$  is a parameter which depends on the sensitivity and noise characteristics of the thermometer and can have values between 1.2 and 2.0.

The energy resolution of a semiconductor device is:

$$\Delta E_{FWHM} = 2.35\sqrt{wFE} \sim 110eV \quad (6)$$

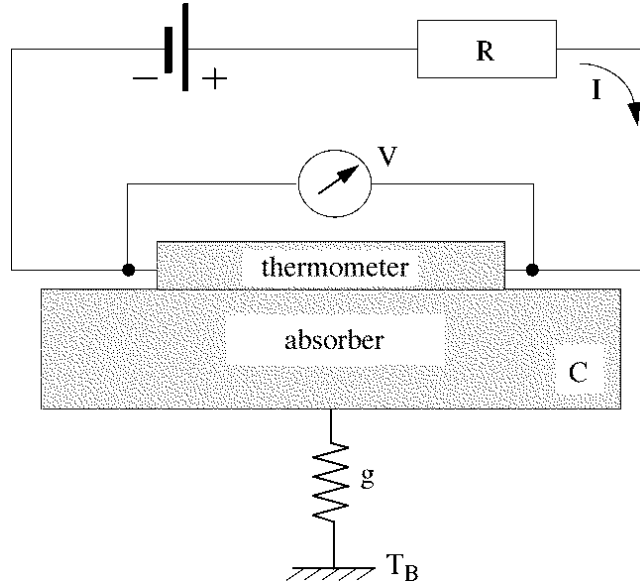


Figure 1. The principle of a cryogenic calorimeter is shown.

for a 6keV x-ray, where  $w$  is the average energy necessary to produce an electron hole pair. It has a typical value of  $w \approx 3\text{eV}$ . The Fano factor is  $F = 0.12$  for Silicon.

The use of superconductors as cryogenic particle detectors was motivated by the small binding energy  $2\Delta \approx 1\text{meV}$  of the Cooper pairs. A particle traversing a superconductor produces quasiparticles (by breaking Cooper pairs) and phonons. As long as the energy of the quasiparticles and phonons is higher than  $2\Delta$ , they break up more Cooper pairs and continue to produce quasiparticles until their energy falls below the threshold of  $2\Delta$ . Thus, compared to a semiconductor, several orders of magnitude more free charges are produced leading to a much higher intrinsic energy resolution.

For a superconducting cryogenic calorimeter with a Cooper pair binding energy of  $2\Delta \approx 1\text{meV}$ , the best obtainable energy resolution is

$$\Delta E_{FWHM} = 2.35\sqrt{2\Delta FE} \sim 3\text{eV} \quad (7)$$

for a 6keV x-ray assuming  $F=0.2$  for most superconductors.

In Fig.2 x-ray spectra obtained with a state of the art Si(Li) solid-state device and a cryogenic microcalorimeter using a HgCdTe absorber are compared. The microcalorimeter was a rather early version developed by the Wisconsin, NASA Goddard group and had an energy resolution of 35eV. In the meantime this group<sup>37</sup> and others<sup>21,40</sup> have succeeded in building microcalorimeters with energy resolutions between 3 and 5eV. Such calorimeters have typically a surface area of  $\leq 1mm^2$  and a thickness of several  $\mu m$ .

## 5 Phonon Sensors

Phonons produced by a particle interaction in an absorber are far from thermal equilibrium. They must decay to lower energy phonons and become thermalized before the temperature rise  $\Delta T$  can be measured. Since thermalisation results in a rather long decay time (order of msec) of the signal pulse, a cryogenic phonon detector cannot tolerate counting rates much higher than a few Hz.

The most commonly used phonon sensors are: Semiconducting thermistors and superconducting transition edge sensors (TES).

### 5.1 *Semiconducting Thermistors*

A thermistor is a heavily doped semiconductor slightly below the metal insulator transition. Good uniformity of doping concentrations can be achieved either with ion implantation or with neutron transmutation doping (NTD). In the latter case, thermal neutrons from a reactor are captured by nuclei which transform into isotopes. These can then be the donors or acceptors for the semiconductor. NTD Ge thermistors are frequently used, because of their reproducibility and their uniformity in doping density. Furthermore they are easy to handle and commercially available. However, they have the disadvantage of being thermal phonon sensors with intrinsically slow response signals and of having to deal with Joule heating.

### 5.2 *Superconducting Transition Edge Sensors (TES)*

An alternative thermometer is a thin superconducting strip which is operated close to its superconducting to normal phase transition temperature  $T_c$ . The operating temperature is chosen so that it is sensitive in the region of the temperature versus resistance diagram as shown in Fig.3a. The voltage drop across the strip, i.e. the signal pulse height, depends on the magnitude of the

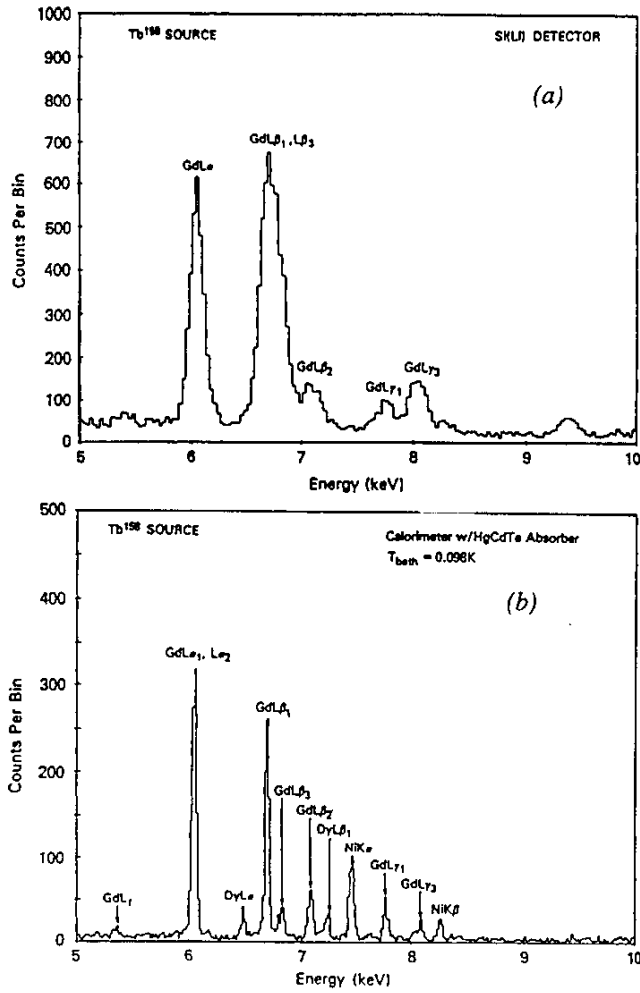


Figure 2. X-ray spectra obtained (a) with a Si(Li) solid state detector and (b) with a HgCdTe micro-calorimeter (from the Wisconsin/Goddard group) are compared.

constant current through the strip and on the change of the resistance  $\Delta R$ . However, the current should be kept as small as possible in order to reduce the self-heating effects. The Munich group<sup>52</sup> has developed a transition edge sensor made out of tungsten (W) with a transition temperature of 15 mK. They used low impedance sensors with normal conducting resistances between 10

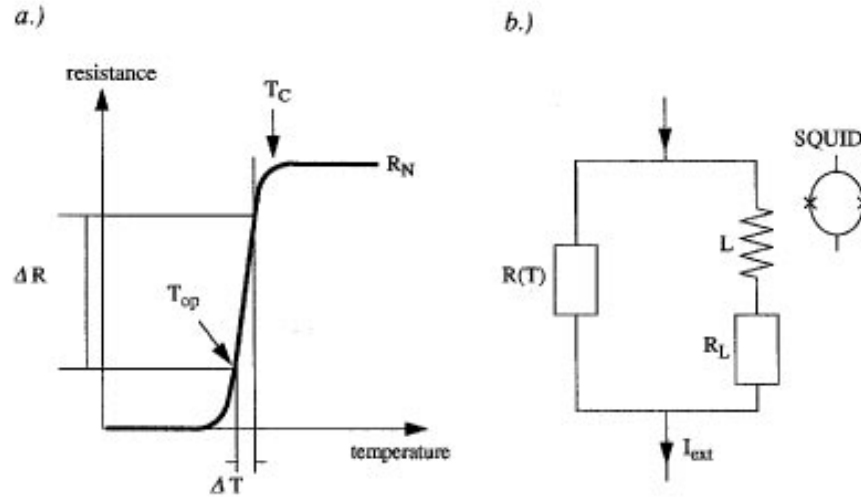


Figure 3. (a) The temperature versus resistance diagram of a superconducting strip close to the transition temperature  $T_c$  is shown. (b) The dc-SQUID readout of a transition edge sensor is shown.

and  $100\text{m}\Omega$ . A constant current is fed through the readout circuit as shown in Fig.3b. An increase in  $R(T)$  due to a temperature rise forces more current through the parallel branch of the circuit, inducing a magnetic flux change in  $L$  which is measured with high sensitivity by a SQUID. However, in this mode the temperature of the detector has to be stabilized with very high precision in order to achieve a good energy resolution. Recently K.D.Irwin<sup>22</sup> has developed an interesting auto-biasing electrothermal feedback system, which works as a thermal equivalent to an operation amplifier. It keeps the temperature of the superconducting strip at a constant value within its transition region. When operating the transition edge sensor in a voltage biased mode ( $V_B$ ), a temperature rise in the sensor causes an increase in its resistance and a corresponding decrease in the current, which results in a decrease of the Joule heating ( $V_B \cdot \Delta I$ ). The feedback uses the decrease of the Joule heating to bring the temperature of the strip back to the constant operating value. Thus the device is self calibrating. The deposited energy in the absorber is given by  $E = -V_B \int \Delta I(t) dt$ .

Other transition edge sensors, made from proximity bilayers such as Al/Ag, Al/Cu, Ir/Au, Mo/Au, and Mo/Cu, have been developed to cover also higher transition temperatures in the range between 15 and 150mK.

TES is sensitive to non-thermal phonons with energies well above  $2\Delta$ . While losing energy these phonons produce quasiparticles before they thermalize. Since this process is very much faster than thermalization, signals of the order of  $\mu\text{s}$  can be achieved, enhancing considerably the counting rate capability of these devices as compared to thermal phonon sensors. Due to this circumstance and the selfcalibrating effect of the electrothermal feedback system, TES are now among the most frequently used devices in calorimetric measurements.

## 6 Quasiparticle Detection

Quasiparticles produced by the absorption of X-rays or the energy loss of a transient particle in a superconducting absorber can be measured with a Superconducting Tunnel Junction (STJ). When biasing the STJ at a suitable voltage the tunneling current through the junction is proportional to the excess number of quasiparticles produced. Arrays of STJs are also used to measure high energy, non-thermal (ballistic) phonons produced in either a dielectric or superconducting absorber. An excellent educational description of STJs can be found in <sup>23</sup>.

### 6.1 Superconducting Tunnel Junctions (STJ)

A STJ consists of two superconducting films with a thickness of typically a few nm separated by a thin, 1-2 nm thick, tunnel barrier, which is usually the oxide of one of the superconductors. Typical junction areas are of the order of  $100 \times 100 \mu\text{m}^2$ . As a quasiparticle detector, the STJ is operated with a bias voltage which is usually set to be less than  $\Delta/e$ . A magnetic field of about 100 Gauss is applied in the plane of the junction in order to suppress the Josephson supercurrent. A change in the number of quasiparticles will lead to a tunneling current which is proportional to the number of quasiparticles produced in the absorber. Since the Poisson statistical fluctuations of the quasiparticle density in the superconductor are very small, the two most important parameters driving the energy resolution of the STJ are the tunneling rate  $\tau_{tunnel}^{-1}$  and the thermal recombination rate  $\tau_{re}^{-1}$ . The temperature dependence of the thermal recombination rate is given by



$$\tau_{re}^{-1}(T) = \tau_0^{-1} \sqrt{\pi} \left( \frac{2\Delta}{kT_c} \right)^{5/2} \sqrt{\frac{T}{T_c}} \exp\left(-\frac{\Delta}{kT}\right) \quad (8)$$

where  $\tau_0$  is the characteristic time of a superconductor. It has the values  $\tau_0 = 2.3\text{ns}$  for Sn,  $\tau_0 = 438\text{ns}$  for Al and  $\tau_0 = 0.15\text{ns}$  for Nb <sup>24</sup>.

The recombination rate  $\tau_{re}^{-1}$  can be minimized when operating the detector at sufficiently low temperatures, typically at 0.1 Tc, where the number of thermally excited quasiparticles is very small. The tunneling time is given by

$$\tau_{tunnel}^{-1} = R_{norm} \cdot e^2 \cdot N_0 \cdot A \cdot d \quad (9)$$

where  $R_{norm}$  is the normal conducting resistance of the junction,  $N_0$  is the density of states of one spin at the Fermi energy,  $A$  is the junction overlap area and  $d$  the thickness of the corresponding film. In practice, the tunneling time has to be shorter than the quasiparticle lifetime. For  $100 \times 100 \mu\text{m}^2$  junctions a tunneling time of the order of  $1\mu\text{s}$  has been obtained. In order to achieve even shorter tunneling times, one would have to try to further reduce  $R_{norm}$ . However, there is a fabrication limit avoiding micro-shorts in the insulator between the superconducting films. Quasiparticles are lost for detection when they produce sub-gap phonons with energies below  $2\Delta$  (which do not contribute to the detector signal) or when they diffuse out of the overlap region of the junction films into the current leads instead of crossing the junction gap. N.Booth <sup>20</sup> proposed a scheme (Fig.4) which allows to recover some of these losses by the use of quasiparticle trapping and in some cases even quasiparticle multiplication. The scheme has been shown to work successfully. The quasiparticles produced in the superconducting absorber  $S_1$  diffuse to the superconducting film  $S_2$  of the STJ with a smaller gap energy  $\Delta_2$ . By falling in that trap they relax to smaller energies by emitting phonons, which could produce additional quasiparticles in the film  $S_2$  (quasiparticle multiplication) if their energy is larger than  $\Delta_2$ . The relaxed quasiparticles cannot diffuse back into the superconductor  $S_1$  because of their lower energy. They will eventually tunnel through the STJ, contributing to the signal. In order for quasiparticle trapping to be effective, superconducting absorber materials with long quasiparticle lifetimes have to be selected (for example Al).

Because of their limited size, STJs have so far not been used in connection with large volume calorimeters. This may, however, change in the near future because large arrays of STJs can be produced by now. The Naples group <sup>42</sup> has recently produced an array of circular shaped STJs.

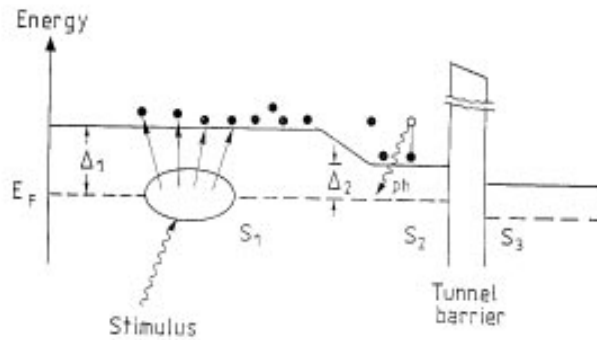


Figure 4. The schematic of quasiparticle trapping is shown. See text for explanation.

STJs are commonly used for high resolution x-ray detection. High energy resolutions of 30 eV for 6 keV x-rays have been obtained by the ESTEC <sup>48</sup> and Livermore <sup>47</sup> groups. As described below, the ESTEC group achieved single photon counting with niobium and tantalum STJs.

### 6.2 Superheated Superconducting Granules (SSG)

Superheated superconducting granules (SSG) have been developed for x-ray imaging, transition radiation, dark matter and solar neutrino detection. A SSG detector consists of billions of small grains (with a diameter of 30 μm for example), diluted in a dielectric material (e.g. Teflon) with a volume filling factor of typically 10%. The detector is operated in an external magnetic field. Metastable type-1 superconductors (e.g. Sn, Zn, Al, Ta) are used, since their phase transitions from the metastable superconducting state to the normal state are sudden (in the order of 100 ns) allowing for a fast time correlation between SSG signals and those of other detectors. The SSG detector is a

threshold detector operated typically at a temperature of  $T=0.1 T_c$ . Its energy threshold is adjustable by setting the external magnetic field at a certain value just below the phase transition border. Particles interacting in a granule produce quasiparticles. While spreading over the volume of the granule the quasiparticles are losing energy via electron-phonon interactions, thereby globally heating the granule up to a point where it may undergo a sudden phase transition (granule flip). The phase transition of individual grains in a large sample can be detected by a pickup loop, which measures the magnetic flux change due to the disappearance of the Meissner-Ochsenfeld effect. The Bern group has developed a readout system which allows to detect single grain flips (grains with  $30\mu\text{m}$  diameter) in a pickup coil of 2cm diameter and 16cm length. As described below, 50 such pickup coils are needed for a 1kg SSG dark matter detector. In parallel, a more sensitive dc-SQUID (Superconducting Quantum Interference Devices) system is under development to increase the sensitivity of the detector by allowing to read smaller size granules<sup>53</sup>.

Small spherical grains can be produced at low cost by industry. Since after fabrication the grains are not of a uniform diameter, they have to be sieved to select the desired size. A grain size selection within  $\pm 2\mu\text{m}$  was achieved.

However, it was discovered that industrially produced grains do not exhibit a sharp phase transition boundary. Their phase transition is smeared by about 20%, leading to an equivalent smearing of the energy threshold. This phase transition smearing could only very recently be reduced by laser treatment and fast cooling of the grains by as much as an order of magnitude<sup>45</sup>. Similar results were also obtained by producing small cylindrical Sn structures on a substrate by evaporation techniques. Both methods seem to allow the production of large quantities of granules for a massive SSG dark matter detector.

A superconducting superheated granule detector offers several unique features: a) The large list of suitable type-1 superconductor materials allows to optimize SSG for specific applications. b) Very low energy thresholds (eV) can be achieved. c) The pickup loop readout system does not dissipate any energy into grains. Therefore the sensitivity of SSG is essentially determined by the grain size and the specific heat of the grain material. d) The sudden phase transitions are beneficial for coincident timing with other signals.

Generally speaking, SSG detectors are among the most sensitive devices to detect very low energy transfers, i.e. nuclear recoils. A detailed description of SSG can be found in<sup>43,44</sup>.

Table 1. WIMP searches with cryogenic calorimeters.

<b>Experiment</b>	<b>Location</b>	<b>Absorber</b>
CDMS	Stanford, U.S.A.	Germanium, Silicium
CRESST	Gran Sasso, Italy	Sapphire
EDELWEISS	Frejus, France	Germanium
MILAN	Gran Sasso, Italy	TeO <sub>2</sub>
ORPHEUS	Bern, Switzerland	Superconducting Sn grains
ROSEBUD	Canfranc, Spain	Sapphire
TOKYO	Nokogiri-yama, Japan	LiF

## 7 Cryogenic Detectors and the Quest for Dark Matter in the Universe

There is evidence that a significant amount of the dark matter in the Universe is of exotic, i.e. non-baryonic, nature. Prime candidates are massive neutrinos, axions and also neutralinos, the lightest SUSY particles predicted by Super Symmetry. But there is plenty of room for other species, which are generally called WIMPs (weakly interacting massive particles).

WIMPs can be detected by measuring the nuclear recoil energy in elastic WIMP-nucleus scattering. Depending on the mass of the WIMP and the mass of the detector nucleus, the average recoil energy can vary between eV and keV. The main advantage of cryogenic devices for the WIMP search is their effectiveness in detecting very low energy nuclear recoils and the possibility to use a large variety of detector materials. The first generation WIMP experiments with cryogenic detectors are being done with absorber masses of about 1kg. Larger detector masses of 100 kg are planned for the future. A list of cryogenic WIMP detectors in preparation or already in operation is given in Table 1.

To be screened from cosmic ray background WIMP detectors are located in deep underground laboratories. In addition they need to be shielded locally against radioactivity from surrounding rocks and materials. The shielding as well as the detector itself have to be fabricated from radiopoor materi-

als. Background suppression by employing only passive shielding in form of radiopoor lead, copper and other materials is expensive and limited in its effectiveness. However, large factors in the detection sensitivity can be gained by using in addition active background recognition methods. Several dark matter detectors make use of this by discriminating between electron recoils (Compton scattering) and nuclear recoils. In this report only a few dark matter detectors are described.

The CDMS collaboration<sup>49,50,51</sup> employs two different techniques to measure the energy loss of a particle in the absorber. The first one utilizes NTD germanium thermistors bonded to Ge crystals. They call this type of detector BLIP (Berkeley Large Ionization and Phonon based detector). The present detector consists of 3 Ge crystals with a weight of 165g each. Each crystal has two thermistor sensors in order to be able to crosscheck the signals rejecting direct particle interactions in one of the thermistors which would yield only small ionisation signals. The detector is operated at a temperature of 20 mK. The event signals are rather slow with risetimes of a few ms and fall times of about 20ms.

The second type detector is called ZIP (Z-sensitive Ionization and Phonon-based detector). It utilizes tungsten aluminum QETs (Quasiparticle trapping assisted Electrothermal feedback Transition edge sensors). This type of sensor covers a large area of the silicon absorber (100g) with aluminum phonon collector pads, where phonons are absorbed by breaking Cooper pairs and forming quasiparticles. The quasiparticles are trapped into a meander of tungsten strips which are used as transition edge sensors. The release of the quasiparticle energy in the tungsten strips increases their resistance, which will be observed as a current change in L detected with a SQUID as indicated in Fig.5. The transition edge device is voltage biased to take advantage of the electrothermal feedback. The signal pulses of the ZIP detector have rise times of a few  $\mu\text{s}$  and fall times of about  $50\mu\text{s}$ . They are much faster than the signals of the BLIP detector since the ZIP detectors are sensitive to the more energetic nonthermal phonons. Their sensitivity to nonthermal phonons and the pad structure of the sensors at the surface of the crystal allows for a localization of the event in the x-y plane (Fig.5).

The energy of the recoiling nucleus or electron in the absorber appears in form of phonons and electron-hole pairs. A simultaneous measurement of both, the phonons and electron-hole pairs, in each event allows to discriminate the nuclear recoils from the electron recoil background events (Fig.6). This is possible since for a given deposited energy the ionization generated by nuclear recoils is smaller than by electrons. By this method 99% of electron recoils with energies above a 15 keV can be recognized.

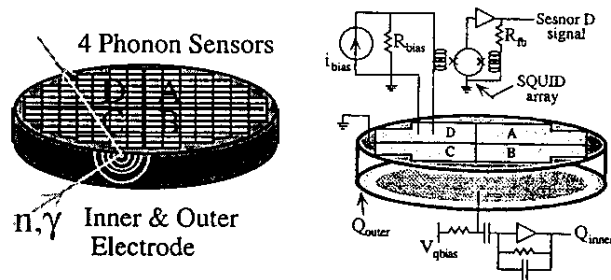


Figure 5. The schematic of the electrical circuits for reading out the phonon and charge signals from a ZIP detector.

The attractive nuclear and electron recoil discrimination applied with the CDMS BLIP detector is also realized in the EDELWEISS experiment, which is presently taking data in the Frejus tunnel at 4800 m.w.e.<sup>55</sup>. The detector uses 70g sapphire crystals. The collaboration plans to increase the detector mass to about 10kg in the future.

The CRESST collaboration<sup>46</sup> is using in the first phase of their dark matter search four 262g sapphire detectors, each equipped with a tungsten TES and electrothermal feedback. The detector is set up in the Gran Sasso Laboratory and operates at a temperature of about 15 mK. The pulse height spectrum measured with a 262g sapphire detector exposed to a x-ray fluorescence source is shown in Fig.7. The large background towards lower energies is attributed to a damaged thin Al sheet meant to absorb Auger electrons from the source. The detector is capable of detecting recoil energies down to about 200 eV.

For the future, the CRESST collaboration<sup>46</sup> is proposing to use  $\text{CaWO}_4$  (Calcium tungstate) crystals as scintillating absorbers. By simultaneously measuring the phonons and the light, they are able to discriminate between nuclear and electron recoils. First results obtained with a 6g  $\text{CaWO}_4$  crystal are shown in Fig.8. The left plot in Fig.8 shows a scatterplot of the energy equivalent of the pulse heights measured in the light detector versus those

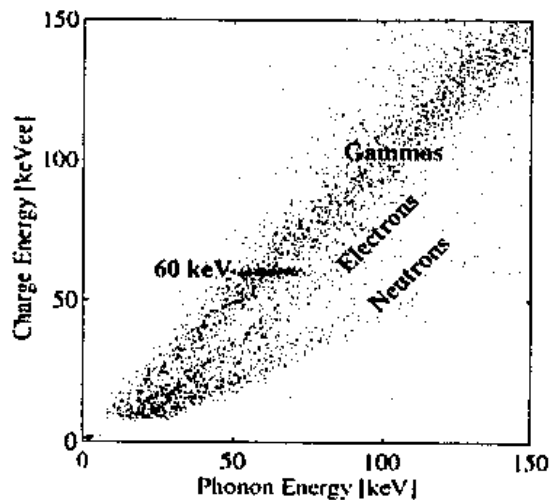


Figure 6. The charge and phonon energy of  $^{14}\text{C}$  electrons,  $^{241}\text{Am}$  photons (60 keV) and  $^{252}\text{Cf}$  neutrons are shown.

measured in the phonon detector. This scatterplot was obtained with an electron and a photon source. The right hand plot shows an additional irradiation with neutrons from an Americium-Beryllium source clearly demonstrating the line coming from neutron induced nuclear recoils. Above an energy of 15 keV 99.7% of the electron recoils can be recognized. At present the CRESST collaboration is investigating also other suitable scintillating materials. With this method a powerful tool of active background rejection can be realized, enhancing the WIMP detection sensitivity of these devices considerably.

The ROSEBUD dark matter experiment consists of two 25g and one 50g sapphire absorbers which are equipped with NTD Ge thermistors. The experiment has recently been set up in the Canfranc Underground Laboratory (Spain) at 2450 m.w.e. and started data taking<sup>56</sup>.

The ORPHEUS collaboration<sup>54</sup> developed a SSG detector for a dark matter search. Nuclear recoil measurements with granules made from type-1 superconductors (Al,Sn,Zn) have been performed in a neutron beam at the Paul

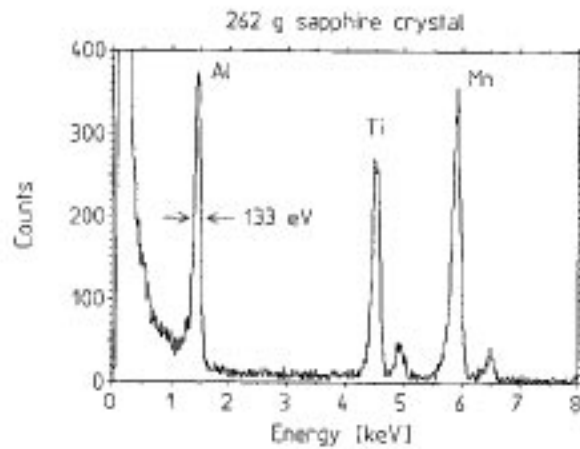


Figure 7. The pulseheight spectrum measured with a 262 g sapphire detector exposed to a X-ray fluorescence source is shown.

Scherrer Institut in Villigen<sup>31</sup>. All these materials turned out to be suitable for a dark matter detector. At present, the ORPHEUS collaboration is setting up a 1kg SSG detector, made from  $30\mu\text{m}$  diameter Sn granules, in the Bern Underground Laboratory at 70 m.w.e. Among other interesting features, as already mentioned above, SSG allows to distinguish ionizing particles which cause many grains to flip from WIMP interactions which cause only one grain to flip. This feature will be used to reduce background from cosmic rays, Compton scatterings and radioactive materials. Fig.9 shows a pulseheight spectrum obtained with a Zn SSG detector exposed to a neutron beam at the Paul Scherrer Institut. The one grain flips are due to neutron scatterings, while the flips of several granules are due to Compton electrons also present in the beam.



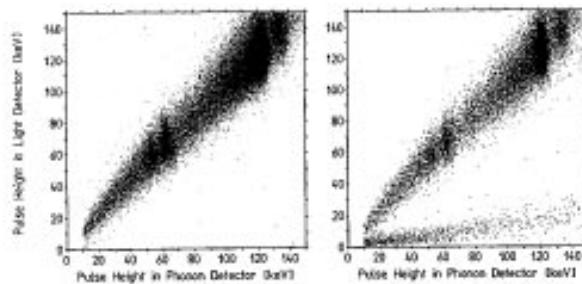


Figure 8. Left, a scatterplot of the energy equivalent of the pulse heights measured in the light detector versus those in the phonon detector. This was obtained with an electron and photon source. Right, the scatterplot with additional irradiation with neutrons from an Americium-Beryllium source is shown, clearly demonstrating the lower line coming from neutron induced nuclear recoils.

## 8 Double Beta Decay Experiments

The largest low temperature detector in operation so far is the one of the Milan group in the Gran Sasso Laboratory. The detector consists of an array of 20  $\text{TeO}_2$  crystals of 340g each, totalling a mass of almost 7kg<sup>25</sup>. Attached to each crystal are Ge NTD thermistor thermometers. The detector is mainly used to search for the neutrinoless double beta decay of  $^{130}\text{Te}$ , taking advantage of the large isotopic abundance (34%) and the large transition energy of 2528 keV. Low temperature devices are particularly well suited for this type of research since they provide energy resolutions better than or comparable with semiconductors and they can be made of a wide choice of double beta active nuclei. The  $\text{TeO}_2$  detector of the Milan group is also used for the search of WIMPs. However, its recoil energy threshold of 13keV is rather high compared

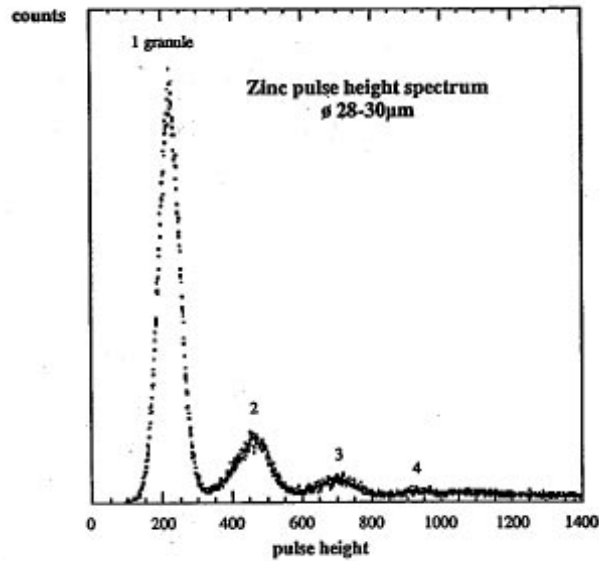


Figure 9. The pulseheight spectrum of a Zn SSG detector exposed to a beam of neutrons and Compton electrons is shown.

to other cryogenic detectors.

For the future E.Fiorini <sup>26</sup> proposes a large Cryogenic Underground Observatory for Rare Events (CUORE) in the Gran Sasso Laboratory. The proposal foresees the construction of a cryogenic detector containing many such crystals ( $\text{TeO}_2$  or others), totalling a mass of about one ton. From this device very important new results on double beta decay, WIMP search, solar axions and neutrino interactions from artificial sources are expected.

## 9 Beta Decay and the Mass of the Electron Neutrino

Most of the experiments to search for a non-zero mass of the neutrino in beta decay are using the tritium decay into  $^3\text{He}$ , since this transition has a rather low endpoint energy of 18.6keV. However, so far no experiment was able to establish a finite mass of the neutrino. Only upper limits were obtained, of which the lowest is 4.35eV <sup>27</sup>. One of the problems with experiments based

on a spectroscopic measurement of the emitted electron is that they all yield negative values for the square of the neutrino mass when fitting the electron energy spectrum. This could possibly be due to final state interactions (like tritium decays into excited atomic levels of  $^3\text{He}$ ), which lead to a deviation of the expected energy spectrum of the electron. Low temperature calorimeters reaching similar energy resolutions could perhaps overcome these difficulties, since they measure the total energy including final state interactions such as the de-excitation energy of excited atomic levels.

The Genova group has studied the beta decay of  $^{187}\text{Re}$  with a cryogenic microcalorimeter <sup>28</sup>. The detector is a rhenium single crystal (2mg) coupled to a Ge NTD thermistor. Rhenium is a superconductor with a critical temperature of 1.7 K. Natural Re contains 62.% of  $^{187}\text{Re}$  with an endpoint energy of about 2.6 keV. The operating temperature of the detector was  $T = 90$  mK. In their first attempt they made a precise measurement of the endpoint energy of  $(2.64 \pm 0.02)$  keV and of the half-life of  $(62 \pm 6) \times 10^9$  years. The Milan group has also started to develop thermal detectors for a  $^{187}\text{Re}$  neutrino mass experiment <sup>29</sup>. With cryogenic calorimeters a higher sensitivity to low neutrino masses may be achievable in the future, provided that an energy resolution of less than 10 eV can be obtained and the statistics at the endpoint energy can be improved. The latter may raise a problem for thermal phonon detectors, since their signals are rather slow and therefore limit the counting rate capability considerably. This problem may be overcome by a new approach reported at this conference <sup>30</sup>, which uses the fast transition of Re from a metastable superconducting into a normal state.

With their Re cryogenic microcalorimeters the Genova group was able to detect interactions between the emitted beta particle and its local environment, known as beta environmental fine structure <sup>32</sup>. Their encouraging results show that cryogenic microcalorimeters may also offer a new way to study molecular and crystalline structures.

## 10 Single Photon Counting Cryogenic Detectors for Applications in Astrophysics

A detector capable of measuring individual photons with high efficiency for a wide range of wavelengths (optical to near infrared) and at the same time the arrival time of every single photon falling upon the detector has so far not existed. However, as recently demonstrated by the ESTEC (European Space Agency) group, superconducting tunnel junctions can be used as single photon counting spectroscopic detectors <sup>33</sup>. The detection principle is based on the fact that for a superconductor with a  $\approx 1$  meV gap energy an optical photon

of  $\approx 1\text{eV}$  represents a large amount of energy. Thus a photon impinging on a superconductor, like for example tantalum, can create many quasiparticles leading to a measurable tunnel current across a voltage biased junction. The tantalum STJ developed by the ESTEC group is shown in Fig.10. The device consists of a  $20 \times 20\mu\text{m}^2$  and 100nm thick epitaxial tantalum film on a sapphire substrate with a 30nm thick aluminum trapping layer on top. The tunnel barrier is 1 nm thick and consists of oxidized aluminum. Quasiparticles produced after photoabsorption in the tantalum layer will be trapped by the aluminum film close to the barrier. The initial fluctuation in the number of charge carriers created by photoabsorption combined with the tunnel noise leads to an overall limiting resolution of a junction in terms of wavelength. In Fig.11 the resolution obtained with tantalum and niobium based devices are shown <sup>34</sup>. Also shown is the expected performance of molybdenum and hafnium STJs, which are also under development by the ESTEC group. The obtained quantum efficiency for the tantalum STJ is 70% for wavelengths of 200-600nm with a cutoff below 200 nm due to the sapphire substrate. It is possible to extend the short wavelength limit to 110 nm by replacing the sapphire substrate with magnesium fluoride. The reflectivity of the sapphire substrate and the tantalum reduces the quantum efficiency in the infrared considerably, a feature which can be used as an infrared filter for some applications.

A cryogenic camera consisting of STJ pixel arrays is an attractive device for astronomical observations . The single photon detection capability allows to observe very faint and distant objects and to determine their distance through red shift. A cryogenic camera with a 6x6 array of tantalum STJ's (with a pixel size of  $25 \times 25\mu\text{m}^2$ ) has been recently (Feb.1999) installed in the William Herschel Telescope on La Palma. For a first proof of principle of this novel technique, the telescope was directed towards the Crab pulsar, whose already known periodicity of 33ms was measured by the cryogenic camera as shown in Fig.12 <sup>35</sup>. The photon arrival time information was recorded with an accuracy of about  $5\mu\text{s}$  with respect to GPS timing signals. The results nicely demonstrate the capabilities of this technology for future astrophysical observations.

## 11 Microcalorimeters for X-ray Astronomy

Cryogenic microcalorimeters provide major improvements over conventional detection systems in x-ray astronomy. For example gratings and Bragg crystal spectrometers have an excellent energy resolution, but at the expense of a very small acceptance and energy range. Scanning over an entire x-ray spectrum (0.05 to 1keV) of an extended source requires very long and expen-

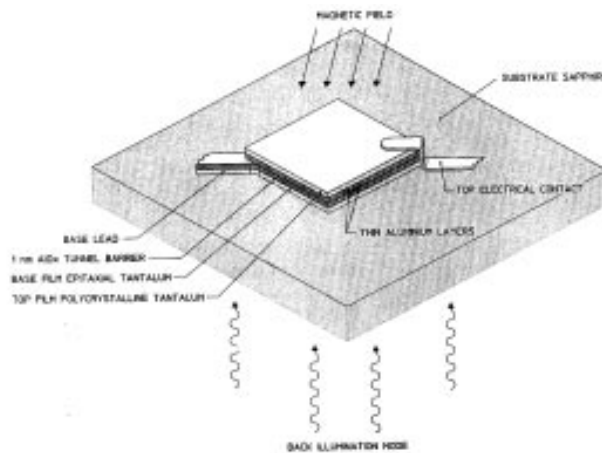


Figure 10. The schematic of the tantalum tunnel junction is shown. The orientation of the magnetic field (parallel to the junction) to suppress the Josephson current is indicated.

sive observation times . On the other hand solid state detectors with large angular acceptance do not reach energy resolutions better than 100eV. In contrast cryogenic microcalorimeters can measure the energy of each incident x-ray, simultaneously covering the entire energy range of interest. In addition they have no limitation on the acceptance angle. However the deployment of cryogenic detectors for experiments in space poses a new technical challenge. Pioneering work in this direction has been done by the Wisconsin, Maryland, NASA Goddard (WMN) group <sup>36,57</sup>.

The WMN group has developed a microcalorimeter array consisting of 36 0.5mmx2mm x-ray detectors with ion implanted silicon thermistors and HgTe absorbers. The microcalorimeters are operated at 60mK. The cryostat consists of an adiabatic demagnetization refrigerator inside a four liter liquid helium dewar. The cryogenics together with the detector fit into a cylinder of about 35 cm diameter and 40 cm length. The detector was flown on a suborbital sounding rocket to observe the interstellar diffuse x-ray background

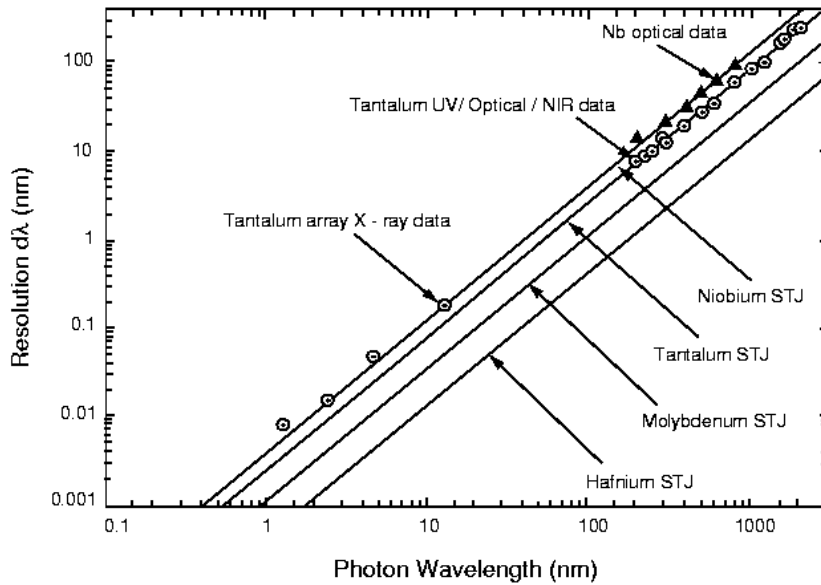


Figure 11. The resolution of tunnel junctions made from superconductors as a function of wavelength is shown.

in the range of 0.05 to 1keV. The sounding rocket reached an altitude of about 235km. The flight provided 240s of observation time above 165km, enough to make reasonable spectroscopic measurements. During observation the Helium bath temperature was regulated to better than  $1\mu\text{K}$ . The energy resolution obtained on single pixels ranges from 3.8 - 4.8eV FWHM<sup>37</sup>. When recovering the payload after the flight the dewar contained still some liquid helium.

The physics of the diffuse interstellar x ray background is not very well understood. It seems that a large component is due to collisional excitations of particles in an interstellar gas with temperatures of a few  $10^6\text{K}$ . A detailed spectral analysis would allow to determine the physical state and the

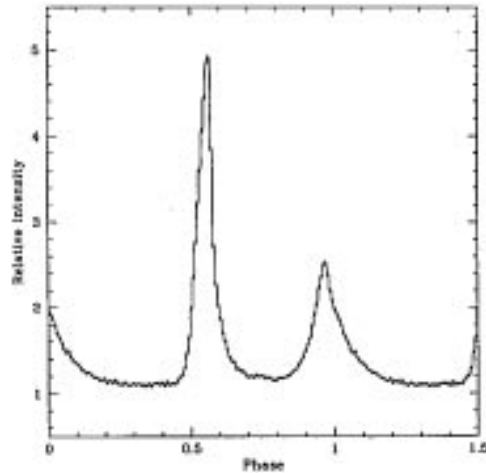


Figure 12. The pulse profile for the Crab pulsar from the 6. Febr. 1999 data over the wavelength range 310-610 nm (128 phase bins) is shown.

composition of the gas. Since the interstellar gas occupies a large fraction of the volume within the galactic disc, it plays a major role in the formation of stars and the evolution of the galaxy. By employing a conical foil mirror in front of the microcalorimeters the WMN group is also planning to perform spectroscopic observations of supernova remnants in the near future.

## 12 Transition Edge Microcalorimeters for Industrial Applications

A group of the National Institute of Standards and Technology (NIST) in Boulder, Colorado (USA) has developed high performance x-ray microcalorimeters based on superconducting transition edge sensors (TES) <sup>38</sup>. The detectors are cooled to 70 mK by a compact adiabatic demagnetization refrigerator and can be mounted on a scanning electron microscope. These devices have features which make them very attractive for industrial appli-

cations in x-ray microanalysis. For example the excellent energy resolution of these devices enables to measure the chemical shifts in the x-ray spectra caused by changes in the electron binding due to chemical bonding. Another application is the analysis of contaminant particles and defects for the semiconductor industry. This technology looks also promising to be used in detecting accelerated large masses such as proteins and DNA in a spectrometer. This method would allow to make DNA sequencing several orders of magnitude faster than current gelelectrophoresis methods<sup>41,39</sup>.

The main advantage of microcalorimeters as compared to more conventional x-ray detection systems (Bragg spectrometers and solidstate detectors) is their ability to cover the entire x-ray spectrum of interest simultaneously and to resolve the closely spaced lines with high resolution. However, microcalorimeters are intrinsically slow devices with limited counting rate capabilities and with small effective surfaces. To cope with these problems the NIST group has developed the following improvements. They are using TES sensors with an electrothermal feedback system which allows to decrease the time it takes for the microcalorimeter to reach thermal equilibrium. This way a gain in counting rate of up to a factor 100 could be achieved. To compensate for the small detector surface they developed an x-ray focussing device using polycapillary optics. The device consists of many fused tapered glass capillaries which focus the x-rays by means of internal reflection onto the microcalorimeter increasing its effective area. The excellent performance of the NIST microcalorimeter as compared to a Si(Li) solid state device is clearly demonstrated in Fig.13. The microcalorimeter has an energy resolution of 3eV, an effective surface area of 4mm<sup>2</sup> and a count rate capability of 1000 per second. A cross sectional view of a TES microcalorimeter developed by the NIST group is shown in Fig.14. Currently the NIST researchers are working on further improving the energy resolution and the counting rate capability of their calorimeters. Nevertheless they already demonstrated the quality of these devices for industrial and other applications.

### 13 Conclusions

Cryogenic detectors allow to explore new domains in physics and astrophysics which have sofar not been so easily accessible with other devices. The physics of cryogenic detectors, however, is more complicated than that of ionization devices, therefore rather long research and development times are required. The cryogenic technology is very advanced and commercially available. It allows to perform experiments underground and in future even in orbit. Massive (several kg) cryogenic detectors for dark matter and double beta decay



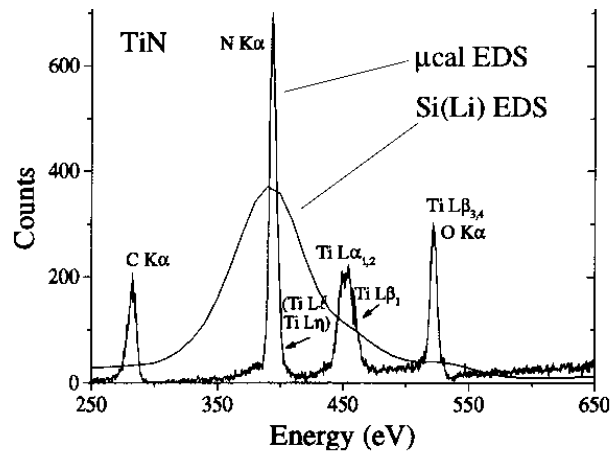


Figure 13. The energy resolution of a Si(Li) solid state device versus a energy dispersive (EDS) micro-calorimeter is shown on the example of TiN, where TiN is an important interconnect and diffusion barrier used in the semiconductor industry.

experiments are already in operation. For the future detectors with 100 kg mass and beyond are planned. The application of cryogenic detectors in other fields of research as well as in industry has been growing rapidly in the last years.

Enjoying the warm and sunny weather in Lisbon one easily forgets that there are things which work better in the cold.

### Acknowledgments

I would like to express my very special gratitude to Amelia Maio and the organizers of this conference for the excellent work they have done to make this conference a great success. My warmest thanks also to S.Janos for the many enlightening discussions during the preparation of this talk and for his careful reading of this manuscript. Furthermore I would like to thank

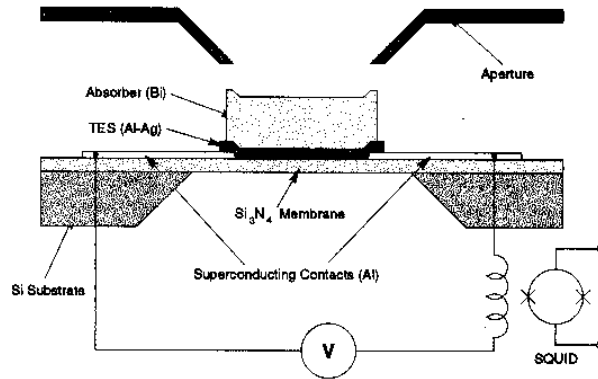


Figure 14. The cross-sectional view of the TES micro-calorimeter is shown. The X-rays are passing through an aperture and are absorbed in the Bi film.

R.Cristiano, E.Fiorini, R.Gaitskell, G.Hilton, H.Hoevers, D.Mac Cammon, T.Peacock, F.Proebst, B.Saduolet and D.Wollman for providing me with material for this talk. This work was supported by the Swiss National Science Foundation.

## References

1. Simon F., Nature 135 (1935) 763
2. Andrews D.H. et al., Phys.Rev. 76 (1949) 154
3. Wood G.H., White B.L., Appl.Phys.Lett. 15 (1969) 237 and Can.J.Phys. 51 (1973) 2032
4. Bernas H. et al., Phys.Lett. A 24 (1967) 721
5. Drukier A. and Vallette C., NIM 105 (1972) 285
6. Niinikoski T.O., Udo F. CERN NP Report 74-6 (1974)
7. Fiorini E., Niinikoski T.O., NIM 224 (1984) 83

8. Drukier A., Stodolsky L., Phys.Rev. D 30 N11 (1984) 2295
9. Pretzl K., Schmitz N., Stodolsky L., eds. Low-Temperature Detectors for Neutrinos and Dark Matter. Berlin: Springer-Verlag (1987)
10. Gonzalez-Mestres L., Perret-Gallix D., eds., Low-Temperature Detectors for Neutrinos and Dark Matter II. Gif-sur-Yvette, France: Ed. Frontieres (1988)
11. Brogiato L., Camin D.V., Fiorini E., eds., Low-Temperature Detectors for Neutrinos and Dark Matter III. Gif-sur-Yvette, France: Ed. Frontieres (1989)
12. Booth N.E., Salmon G.L., eds., Low-Temperature Detectors for Neutrinos and Dark Matter IV. Gif-sur-Yvette, France: Ed. Frontieres (1992)
13. Labov S.E., Young B.A., eds., Proc. 5th Int. Workshop on Low Temp. Detectors LTD5, Berkeley, CA. J.Low-Temp.Phys. 93(3/4) (1993) 185-858
14. Ott H.R., Zehnder A., eds., Proc. 6th Int. Workshop on Low Temp. Detectors LTD6, Beatenberg/Interlaken, Switzerland. Nucl.Instrum.Methods A 370 (1996) 1-286
15. Cooper S. ed., Proc. 7th Int. Workshop on Low Temp. Detectors LTD7, Munich, Germany
16. Barone A. ed., Proc. Superconductive Particle Detectors, Torino 26-29 Oct 1987, World Scientific
17. Barone A., Nucl.Phys. B (Proc.Suppl.) 44 (1995) 645;
18. Twerenbold D., Reports on Progress in Physics 59 (1996) 349;
19. Kraus H., Supercond.Sci.Technol. 9 (1996) 827;
20. Booth N., Cabrera B. and Fiorini E. Annu.Rev.Nucl.Part.Sci. 46 (1996) 471
21. Alessandrello A. et al., Phys.Rev.Lett. 82 (1999) 513
22. Irwin K.D., Appl.Phys.Lett. 66 (1995) 1998
23. Barone A. and Paterno G., 1984 Physics and Applications of the Josephson Effect (New York: Wiley)
24. Kaplan B. et al., Phys.Rev. B 14 (1976) 4854 and Erratum Phys.Rev. B 15 (1977) 3567
25. Alessandrello A. et al., Phys.Rev. B ... (in press)
26. Fiorini E., Physics Reports 307 (1998) 309
27. Belesev A. et al., Phys.Lett. B 350 (1995) 263
28. Fontanelli F. et al. NIM A 370 (1996) 247
29. Alessandrello A. et al., Nucl.Phys. B (Proc.Suppl.) 70 (1999) 230-232
30. Gomes M.R. et al., see Proceedings of this Conference
31. Abplanalp M. et al., NIM A 360 (1995) 616
32. Gatti F. et al., Nature Vol.397 (1999) 137

33. Peacock T. et al., *Astron.Astrophys.Suppl.Ser.* 127 (1998) 497
34. Poclart A. et al., *SPIE* 2808 (1996) 523
35. Perryman M. et al., *ESLAB* 1999/021/SA
36. Deiker S. et al., in *Proc. 7th Int. Workshop on Low Temp. Detectors LTD7*, Munich, Germany, S.Cooper ed, C4 (1997) 108
37. Mc Cammon D., private communication
38. Ladbury R. in *Physics Today* (July 1998) 19 and references therein
39. Hilton G. et al., *Nature* 391 (1998) 672
40. Hilton G. private communication
41. Twerenbold D., *NIM A* 370 (1996) 253
42. Cristiano R. et al., *Appl.Phys.Lett.* 74, N 22 (1999)
43. Pretzl K., *Particle World* Vol.1, No.6 (1990) 153
44. Pretzl K., *Journ.of Low Temp.Physics*, Vol.93, No.3/4 (1993) 439
45. Calatroni S. et al., to be published in *NIM*, the *Proceedings of LTD-8* (1999)
46. Bravin M. et al., *MPI-PhE/98-22*
47. Labov S. et al., *Proceedings LTD-7*, editor S.Cooper (1997) 82
48. Peacock T. et al., *Astron.Astrophys.Suppl.Ser.* 123, (1997) 581
49. Nam S. et al., *Proceedings LTD-7*, editor S.Cooper (1997) 217
50. Gaitskell R. et al., *Proceedings LTD-7*, editor S.Cooper (1997) 221
51. Hellmig J. et al., to be published in *NIM*, the *Proceedings of LTD-8* (1999)
52. Colling P. et al., *NIM A* 354, (1995) 408
53. van den Brandt et al., *Nucl.Physics B (Proc.Suppl.)* 70 (1999) 101
54. Abplanalp M. et al., *NIM A* 370 (1996) 227
55. De Bellefon A. et al., *Astroparticle Physics* 6 (1996) 35
56. Cebrian S. et al., *Astroparticle Physics* 10 (1999) 361
57. Kibourne Stahle K. et al., *Physics Today* August 1999, page 32